

# Robust Image Similarity Measurement based on MR Physical Information

Sung-Jong Eun<sup>1</sup>, Eun-Young Jung<sup>2</sup>, Dong Kyun Park<sup>3</sup> and Taeg-Keun Whangbo<sup>4</sup>

<sup>1</sup>Department of Computer Science  
Gachon University, Sujung-Gu, Seongnam, Gyunggi-Do, Korea  
[e-mail: asclephios@naver.com]

<sup>2</sup>Health IT Research Center, Gachon University Gil Medical center, Incheon, Korea  
[e-mail: eyjung@gilhospital.com]

<sup>3</sup>Health IT Research Center, Gachon University Gil Medical center, Incheon, Korea  
[e-mail: pdk66@gilhospital.com]

<sup>4</sup>Department of Computer Science  
Gachon University, Sujung-Gu, Seongnam, Gyunggi-Do, Korea  
[e-mail: tkwhangbo@gachon.ac.kr]

\*Corresponding author: Taeg-Keun Whangbo

*Received September 27, 2016; revised December 14, 2016; revised April 30, 2017; accepted May 25, 2017;  
published September 30, 2017*

---

## Abstract

Recently, introduction of the hospital information system has remarkably improved the efficiency of health care services within hospitals. Due to improvement of the hospital information system, the issue of integration of medical information has emerged, and attempts to achieve it have been made. However, as a preceding step for integration of medical information, the problem of searching the same patient should be solved first, and studies on patient identification algorithm are required. As a typical case, similarity can be calculated through MPI (Master Patient Index) module, by comparing various fields such as patient's basic information and treatment information, etc. but it has many problems including the language system not suitable to Korean, estimation of an optimal weight by field, etc. This paper proposes a method searching the same patient using MRI information besides patient's field information as a supplementary method to increase the accuracy of matching algorithm such as MPI, etc. Unlike existing methods only using image information, upon identifying a patient, a highest weight was given to physical information of medical image and set as an unchangeable unique value, and as a result a high accuracy was detected. We aim to use the similarity measurement result as secondary measures in identifying a patient in the future.

---

**Keywords:** Image Similarity, R2-map, Texture Analysis, Similarity Distance, MR Physical Information

---

This study was supported by a grant of the Korea Health Technology R&D Project through the Korea Health Industry Development Institute (KHIDI), funded by the Ministry of Health & Welfare, Republic of Korea (grant number HI14C3201)

## 1. Introduction

Recently, introduction of the hospital information system has remarkably improved the efficiency of health care services within hospitals. However, each hospital uses a different system, and the types of information collected are different, which causes difficulties in exchanging medical information among hospitals. Consequently, a problem of inefficiency emerges. For example, a patient who wants to treat the same disease in another hospital needs to take examinations and receive diagnosis all over again. As it is time- and money-consuming, in the U.S., patient information of different hospitals is compared and analyzed through MPI (Master Patient Index) algorithm, and when patient's information is used cross hospitals, an individual patient is identifiable. It improves the quality of hospital care and at the same time, time and money are less wasted. To improve health care services, the major and crucial problem, integration of medical information among hospitals, should be solved, and as a preceding step, studies on patient identification algorithm to search the same patient among different hospitals should be carried out. Patient information identification can be done by measuring similarity comparing various fields of individual's basic information including patient's name, address, etc. and treatment information including disease history, etc. In order to increase the accuracy of patient information identification algorithm such as MPI, etc., this paper intends to use this method as a supplementary method for overall similarity measurement algorithm considering patient's medical image similarity measurement as secondary measures. The conventional general image matching method processes data based on grayscale image information. Thus, for the case that images are matched although the boundaries of pixels are ambiguous or gray values themselves are different in the regions, there have been many limitations in the analysis method. In order to solve the limitations of the conventional image matching method, this paper aims to propose an algorithm with a high accuracy even in various imaging conditions by utilizing MR physical information together. The greatest feature of the proposed method is the use of MR physical information, and a higher accuracy was calculated compared to typical image matching methods utilizing only the conventional grayscale information. In this paper, the proposed algorithm is described step-by-step in each chapter.

## 2. Related Work

Query methods generally supported for the image search system are utilized in medical image similarity measurement [1]. The types of queries supported include text keyword query and sketch query in which a user can create a query using pre-defined disease icons and template images. The text keyword query is a keyword-centered query method used in the general search system and is used in the situation where a database for patient's brain MRI and information is constructed. The sketch query is a query method in which a user draws the shape of the object, color, and screen layout of the query image that the user wants to query in a direct operation method. However, brain MRI has a disadvantage in that it is very difficult to create query images using image editing tools because the attribute values of objects consisting images are very small and the relationships among the objects are complex. Besides these, there are methods comparing image information only. In general, there are methods comparing global or local region similarity using image processing method. The methods comparing similarity between regions are diverse including texture analysis method [2], an analysis method using Wavelet [3], an analysis method extracting shape information such as edges[4], etc. In addition, there is a SWI(Susceptibility Weighted Imaging)[5-10] that

improving accuracy by utilizing a method of emphasizing gray scale information in preprocessing stage. However, these methods have a problem that incorrect results may be obtained when the distribution of the brightness values of the pixels or the type of connection is similar because these methods process information only with general gray scale image information.

### 3. Proposed Image Similarity Measurement Method

In this paper, to solve the problem that incorrect results are derived due to limited image information when image similarity is measured by aforementioned general image processing, R2-map information is used additionally as a MR's physical approach. The proposed method is processed by following procedure.

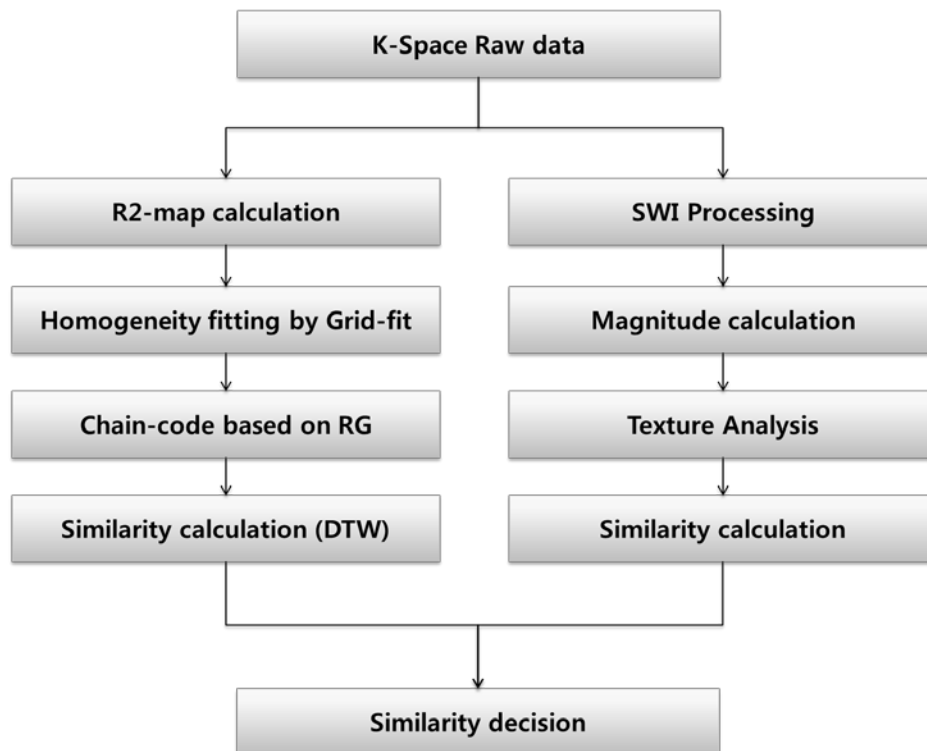


**Fig. 1.** Overview of the proposed method

Like (Fig. 1), the whole process of this paper starts from K-space data. Analyses are performed in roughly two ways from the measured K-space data, and the analysis results are used as an important feature of the similarity calculation. As the first feature, R2-map is calculated in K-space data, and the distribution of iron (Fe), which is the feature information that the individual patient has in a specific region, is calculated. Then, to have homogeneity for detection of significant R2-map, grid-based fitting is processed. To detect the region of interest (ROI), after creating a magnitude image in K-space data, the task of separating the object from the background is processed. In the detected ROI, the seed point based on moment information is set, and the similarity of pixels is measured through the region growing method and saved in the chain code method. Later, the similarity between the image entered through DTW and the image in the DB is calculated. As the second feature, the similarity is measured

by texture analysis. For this, by applying SWI, which is an image improvement method based on MR physics, an efficient image improvement task is processed without being affected by contrast to the magnitude image and brightness conditions. Through comparison of the feature values for textures between the improved image and the image in DB, the second similarity is calculated. Lastly, by applying the weights of the similarity calculated through R2-map and texture analysis, the final similarity is calculated to determine if the images belong to an identical patient. This paper addresses an image matching algorithm that is applied to the image search system. The advantage of the proposed algorithm is to have a high accuracy in various imaging conditions by utilizing physical information of MR image itself besides the conventional grayscale-based imaging information.

### 3.1 Image Similarity Measurement based on R2-map

#### 3.1.1 Calculation of R2-map

In MR image, the methods are used to distinguish differences from normal tissues through factors such as spinlattice, T1, spin-spin, T2, relaxation times, etc. In this paper, T2-based sequence is used; experimental data are MR images of rats; and R2-map value is obtained by calculating T2-map. Images are acquired using FSE (Fast Spin Echo) sequence, and to calculate T2-map, like the formula (1), Signal Intensity (SI) is calculated [11].

$$SI = SI_0(\exp(-T_E / T_2)) \quad (1)$$

The scan parameters utilized for T2-map calculation were TR / TE : 3 000 / 30 ms, NE (number of echo) : 8, and slices : 24, and the resolution was set to 280 x 280. Employing the parameters, T2-map was calculated by the following formular (2) [12].

$$T_2 = -\frac{T_E}{\ln\left(\frac{SI(T2W)}{SI(PD)}\right)} \quad (2)$$

By taking the reciprocal of the calculated T2-map (1/T2), R2-map can be calculated. In general, T2 value appears to differ depending on the iron (Fe) content of the tissue. Although individual differences somewhat exist, generally T2 values in the tissues containing a large amount of the Fe are yield relatively lower than other signals and noises. Therefore, conversely R2 values are evenly distributed with significantly high values. This paper suggests a R2-map information-based method as most meaningful feature information for comparison of similarity. The following figure shows a sample picture of R2-map calculation.

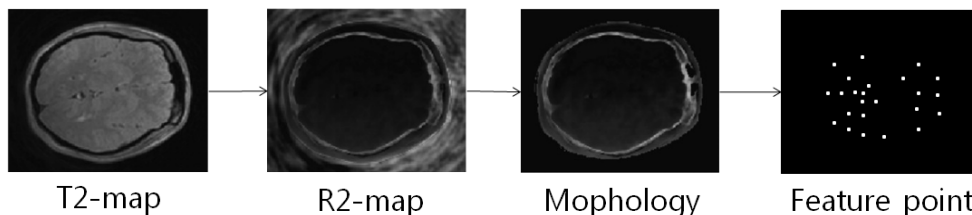


**Fig. 2.** Concept of the R2-map process

### 3.1.2 Homogeneity Fitting by Grid-fit method

In order to perform the fitting operation while maintaining the uniformity of calculated R2-map, this paper uses the method applying a least-square fit for each grid of the image, and it was expressed in the name of grid-fit. We assume that the phase data is spatially smooth and use a Grid-fit method. We propose a more robust and simple phase unwrapping method. The key to our method is to begin the iteration at each grid with least-square fitting by using MiP (Median intensity Projection) process at each axis pixels. Our scheme as the Grid-fit method described in Fig. 3. The steps on the proposed Grid-fit method are:

1. Compute phase image in MR T2 scan raw data.
2. Divide by KxK Grid-regions, that Grid-region size can changeable depend on phase image resolution. Sample Grid-region size K is 6 according to Fig. 2.
3. Compute MiP value at each axis pixels.
4. Adjust the Least-square fitting by using MiP values.
5. Fill median value in each pixel by fitted values at local grid.
6. After fit the local grid, adjust the gaussian filtering at entire Grid-region to enhance the global inhomogeneity.

Fig. 3. Steps on the Proposed Grid-fit

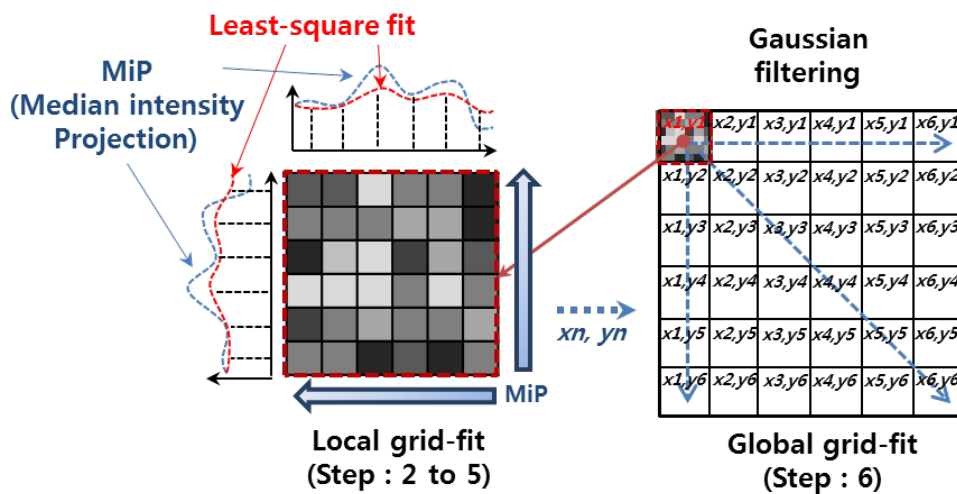


Fig. 4. Processing of Proposed Grid-fit

In this processing method, the basis of the grid region was set to 6X6, and a least-square polynomial expression was solved using a cubic equation. It was treated with a cubic equation to remove spike impulsive noise as well as to have the direction of the minimal intensity. And for the entered values used in the least-square method, the median values of x and y axis in the local grid region were projected, and a representative value for each axis was obtained. Additionally, through the result value of least-square fitting adjusted to each x and y axis, the median value of two values matched to each x and y axis was put as the adjusted local grid-fit result value. In the same way, each grid region is calibrated, and to finally adjust the entire image, the task for mitigating non-uniformity is performed through the Gaussian filter.

### 3.1.3 Dynamic Time Warping(DTW) processing based on chain-code

Region growing is a method of measuring similarities among pixels and expanding and dividing the region. Using one seed point, the similarity of nearby pixels is measured to decide on the seed point. In nearby pixels A and B, the similarity is defined by the following Equation (3).

$$|g(A) - g(B)| \leq \theta \quad (3)$$

In which  $g(A)$  and  $g(B)$  are the gray level pixel values of pixels A and B, and  $\theta$  is the threshold. When the difference between the two pixel values is included in the threshold, there is no pixel similarity and the pixels are combined to grow the region.

In this study, we used not for region division but for the calculation of the chain-code needed for the similarity measurement by DTW. Therefore, the “schema-based” was used. The chain-code is less loss of information about the outline, but the advantage of reducing the storage space, according to any objects such as rotation and size disadvantage of the representation of the object changes. In order to solve the problems with the rotation of the objects, it could make a matching based on the data similar to pixel direction without problem through the aforementioned Region growing method. And the feature point obtained using the closest to the starting point in the two-dimensional moment of the center value of the object extracted by using equation (4-6).

$$M_{pq} = \sum_x \sum_y x^p y^q \text{object}(x, y) \quad (4)$$

$$C_x = \frac{M_{10}}{M_{00}}, C_y = \frac{M_{01}}{M_{00}} \quad (5)$$

$$\text{StartPoint} = \operatorname{argmin}_{x_i \in X, y_i \in Y} \sqrt{(x_i - C_x)^2 + (y_i - C_y)^2} \quad (6)$$

In order to measure the degree of similarity between the two patterns are used for different length DTW. When the feature value of the input image and given a characteristic value of the reference image, the similarity between the length of the other two feature values A, B is used in the equation (7). Problem by varying the degree of similarity and the length of the input pattern is resolved through the normalization, the calculation of the difference value is obtained by using a Euclidean distance.

$$DTW(A, B) = \frac{\gamma(I, J)}{I + J} \quad (7)$$

## 3.2 Texture Analysis based on Susceptibility Weighted Imaging(SWI)

### 3.2.1 Calculation of SWI

SWI [13-17] is a new means to enhance contrast in MR imaging. A number of important tissues have unique magnetic susceptibility differences relative to background or surrounding tissues. we focus on the role of susceptibility, and use the original phase image both by itself

and as a means of altering the contrast in the magnitude images, we refer to this method as SWI. Our goal in this part was to use phase to enhance contrast between tissues with different susceptibilities. All the processing steps involved in the creation of susceptibility weighted magnitude images are schematically summarized in Fig. 4.

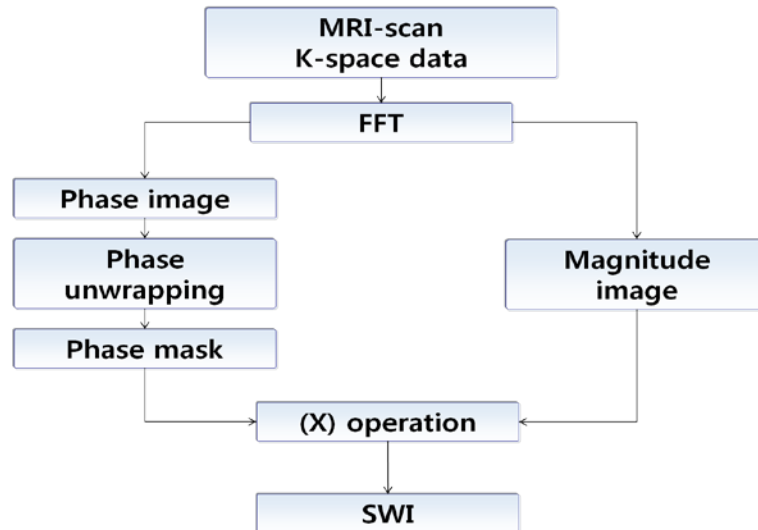


Fig. 5. Overview of the SWI process

Phase unwrapping is a well-studied but long-standing problem outside the field of MRI. Although many different methods of phase unwrapping have been developed, no general solution is available, particularly in the context of MRI. Mathematically speaking, phase unwrapping can be stated simply as recovering the true phase  $\phi$  from its principal or wrapped value  $\phi^{\wedge}$ :

$$\phi = \phi^{\wedge} + k \cdot 2\pi \quad (8)$$

where  $k$  is an integer and, as explained above,  $\phi^{\wedge}$  is limited to a range between  $-\pi$  and  $\pi$  is determined from  $\phi$  through a wrapping operator as follows :

$$\phi^{\wedge} = \mathcal{W}[\phi] \quad (9)$$

This unwrapped phase image is used to create a phase mask that is used to multiply the original magnitude image to create novel contrasts in the magnitude image. The phase mask is designed to suppress those pixels that have certain phases. It is usually applied in the following manner: If the minimum phase of interest is, for example,  $-\pi$ , then the phase mask is designed to be  $f(x)(\phi(x)+\pi)/\pi$  for phases  $< 0$ , and to be unity otherwise, where  $\phi(x)$  is the phase at location  $x$ . That is, those pixels with a phase of  $-\pi$  will be completely suppressed and those with a value between  $-\pi$  and zero phase will be only partly suppressed. This phase mask ( $f(x)$ ) then takes on values that lie between zero and unity. We will refer to it as the negative phase mask. It can be applied any number of times (integer  $m$ ) to the original magnitude image ( $\rho(x)$ ) to create a new

image  $f_m(x)\rho(x)$  with different contrasts[18-19]. Another mask might be defined to highlight positive phase differences by equation 3.

$$\rho(x)_{new} = g^m(x)\rho(x) \quad (10)$$

If the maximum phase of interest is, for example,  $\pi$ , then the phase mask is designed to be  $g(x) = (\pi - \varphi(x)) / \pi$  for phase  $> 0$ , and unity otherwise. We will refer to this as the positive phase mask. And we decide the phase mask multiplication value by some experiments. So we can get the meaningful contrast enhancement image by SWI process.

### 3.2.2 Feature matching based on texture analysis

To measure similarity of texture information, global and local comparison methods are conducted. Global comparison measures roughness, providing texture information[20] which is global and local degrees of roughness, smoothness representing the degree of softness, and entropy value, which is a standard reference indicating irregular randomness. Local comparison is performed by measuring texture information in the patch-based way after dividing the grid areas of ROI. It calculates the degree of similarity information based on the detected texture information. Also, the "patch-based" method is conducted for the general texture analysis on the ROI instead of the global comparison method.

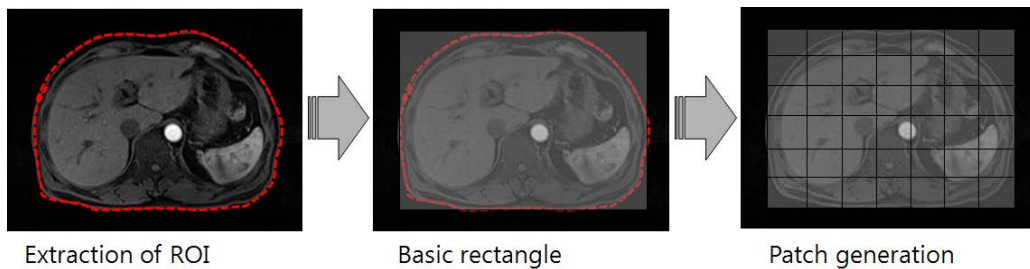


**Fig. 6.** Concept of Patch-based region

The patch information is easily separated into the background and the entity based on the previously analyzed phase unwrapping image, and the patch area is determined through the corresponding entity information. Based on the determined patch area, the roughness, smoothness, and entropy inside the area are analyzed, and then the final image matching rate is calculated. The patch method was conducted for the efficiency and accuracy of processing. **Fig. 6** shows the processing procedure of the patch method in a simple manner.

### 3.3 Similarity Decision

The previously computed R2-map-based similarity measurement result using the degree of similarity of the measurement results with the texture information, measures the final similarity. It was given a high weight of 0.7 when the degree of similarity of the paper measured using R2-map information, and given a weight of 0.3 for texture analysis. This is to have a high accuracy by using the physical information of the degree of similarity is low, the accuracy of a low or ambiguous information of the gray scale image only conventional image

processing method. After giving a weight to two measured values, 0.7 for R2-map and 0.3 for texture analysis comparison, the final result values are calculated and converted to percentages. If the percentage is higher than 90%(0.9), they are concluded to be the same images. And we can summarize the calculation of distance. This can be simply represented with Eq. 11 below.

$$\sum_{g=1}^n (D1_g \times \alpha_1 + D2_g \times \alpha_2) \quad (11)$$

where  $n$  is an total number of test image group,  $g$  is group number,  $D1$  and  $D2$  is distance based on R2-map and texture analysis. And  $\alpha_1$ ,  $\alpha_2$  is a weight value as explained above. The weight for the final result values was determined through experiments. The weight with the highest accuracy for 50 cases under the ratio of 7:3 was selected. Also, the weight of more than 50% was given to the R2-map because the general gray scale images had insufficient or ambiguous information. More weight on physical information led to higher accuracy. For this reason, utilization of physical information was suggested as a key element of the image similarity analysis method.

## 4. Experimental Results and Analysis

An experiment was conducted using a total of 4,500 images information for performance assessment of the proposed method. To evaluate the proposed method, we using the confusion matrix between exist methods. The experiment is described step-by-step in each steps.

### 4.1 Environment of experiment

First of all, the scan parameters utilized for T2-map calculation were TR / TE : 3 000 / 30 ms, NE (number of echo) : 8, and slices : 24, and the resolution was set to 280 x 280. In detail, the parameter was shown as follows [Table 1](#). Also experimental image set was shown as [Fig. 7](#).

**Table 1.** MR Scan Parameters of experiment

Scan parameter	Set value
TR	3,000ms
TE	30ms
Flip angle	20°
Average	1
Matrix	280x280
FOV	20.0x28.0mm
Slice Thickness	1mm
Tesla	1.5T

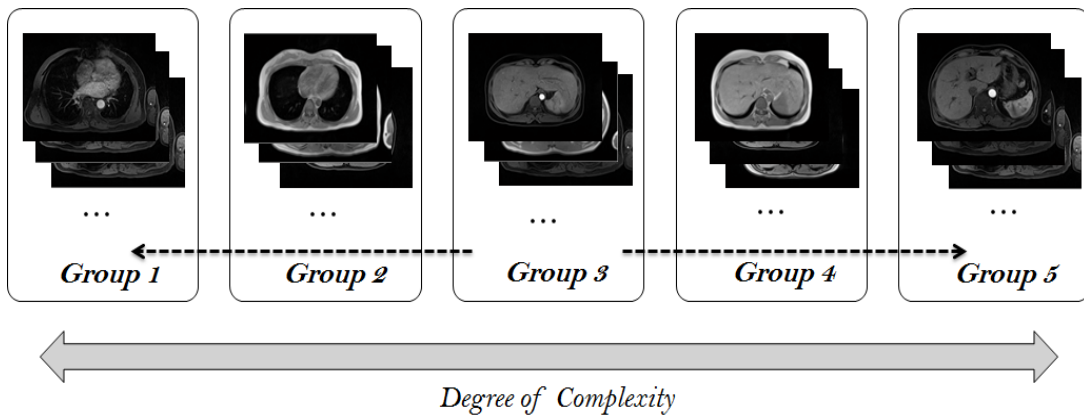


**Fig. 7.** Experiment samples of image set

The other scan parameters was set the flip angle, average, matrix, FOV, slice thickness as following above mentioned. In Experiment image, it was composed of 1,000 abdominal test image include the liver region because of easy to check the unique R2-map information at liver region. That image group was composed of five groups and we do the performance evaluation using similar images that has complexity. In order to increase the accuracy, we do making the five groups by using co-occurrence [21] matrix process due to image pattern is too various even though the same person. In experiment of evaluation, we do the compare proposed method with general exist two methods of texture-based [20] and wavelet [22] algorithm. To evaluate the medical data analysis algorithm, it apply the confusion matrix in positive(matched) group and negative(unmatched) group. And the comparison process was represented as follows **Fig. 8.**

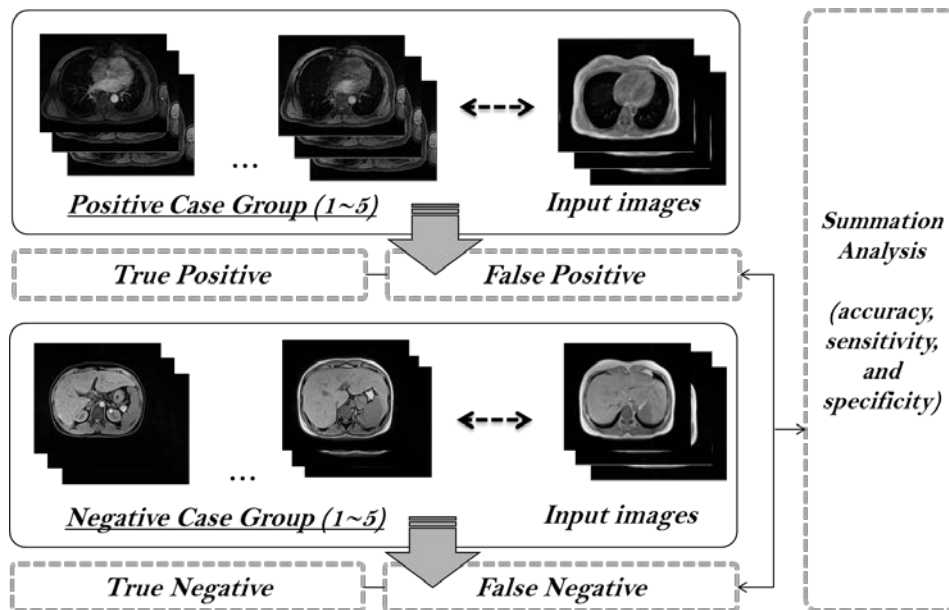


**Fig. 8.** Concept of comparison process

## 4.2 Comparison of performance

In order to experiment, we using the confusion matrix. Using the matrix, the accuracy, sensitivity, and specificity of the suggested algorithm and the typical algorithm were compared. The true positive (TP), false positive (FP), false negative (FN), and true negative (TN) are defined as follows [Fig. 9](#).

\*TP: The matched person is determined as the correct person.  
 \*FP: The matched person is determined as the wrong person.  
 \*TN: The unmatched person is determined as the wrong person.  
 \*FN: The unmatched person is determined as the correct person

**Fig. 9.** Criteria of confusion matrix

The confusion matrix was calculated as average results follows [Table 2](#). And the samples of test was represented as follows [Table 3](#) and [Table 4](#).

**Table 2.** Average results of comparison of the proposed method with the other exist methods

Confusion matrix	Proposed method	Texture based [23]	Wavelet based [25]
True Positive	45(45.4)	21(20.6)	40(40.2)
False Positive	5(4.6)	29(29.4)	10(9.8)
True Negative	45(45.0)	41(40.6)	41(41.4)
False Negative	5(5.0)	9(9.4)	9(8.6)

According to [Table 2](#), we can show the accuracy, sensitivity, and specificity results following [Table 3](#) and [Table 4](#) in detail.

**Table 3.** Result of the Positive case

Positive Case	Proposed method		TP/FP	Texture based		Wavelet based	
	Average distance			Average distance	TP/FP	Average distance	TP/FP
	DTW	Texture					
Group 1	3.601	8.201	42/8	21.110	19/31	8.153	38/12
Group 2	3.187	8.558	46/4	15.870	22/28	5.874	42/8
Group 3	1.258	5.520	48/2	10.250	24/26	3.114	45/5
Group 4	1.924	7.501	47/3	16.112	21/29	5.774	41/9
Group 5	2.552	9.205	44/6	25.150	17/33	7.562	35/15

**Table 4.** Result of the Negative case

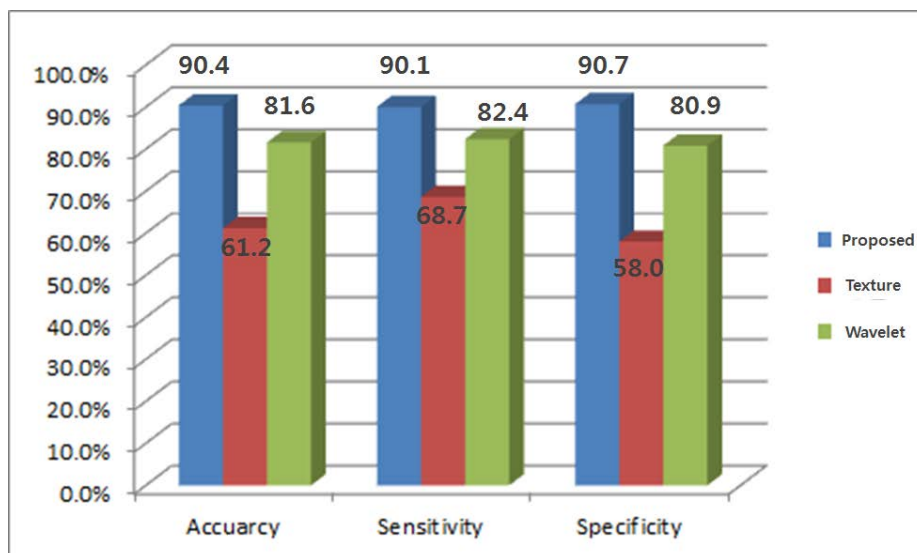
Negative Case	Proposed method			Texture based		Wavelet based	
	Average distance		TP/FP	Average distance	TP/FP	Average distance	TP/FP
	DTW	Texture					
<b>Group 1</b>	45.995	38.112	44/6	35.220	40/10	35.510	42/8
<b>Group 2</b>	44.220	32.520	45/5	35.150	40/10	31.550	40/10
<b>Group 3</b>	40.147	30.220	47/3	32.551	38/12	30.144	40/10
<b>Group 4</b>	43.120	30.780	46/4	33.220	42/8	32.414	41/9
<b>Group 5</b>	42.577	31.550	43/7	35.147	43/7	33.512	44/6

According to calculate the confusion matrix, the formula for defining the confusion matrix factors and for achieving accuracy, sensitivity, and specificity can be as follows **Fig. 10**. The following **Fig 11**. show the accuracy, sensitivity, and specificity results.

$$Accuracy = (TN + TP) / (TN + TP + FN + FP)$$

$$Sensitivity = TP / (TP + FN)$$

$$Specificity = TN / (TN + FP)$$

**Fig. 10.** Accuracy, sensitivity, and specificity calculation method**Fig. 11.** The results of overall analysis

The confirmation of the calculated confusion matrix and the accuracy, sensitivity, and specificity results showed that the suggested method is more accurate and general in high

magnetic fields than are typical algorithms. The suggested method was found to be more effective with an ROC curve. An ROC curve stands for Receiver Operation Characteristic curve, which is mostly used in medical science and dynamics. An ROC curve is drawn based on the average value of sensitivity and specificity of the measured values. As shown in Fig. 12 below, if the area under the curve is 1, it represents perfect results. If the area is 0.5, the results are not suitable. In addition,  $0.9 < \text{AUC} < 1$  represents very accurate results and  $0.7 < \text{AUC} \leq 0.9$  represents comparatively accurate results. It was found that the suggested ROC curve method led to more accurate results compared to the existing comparison methods.

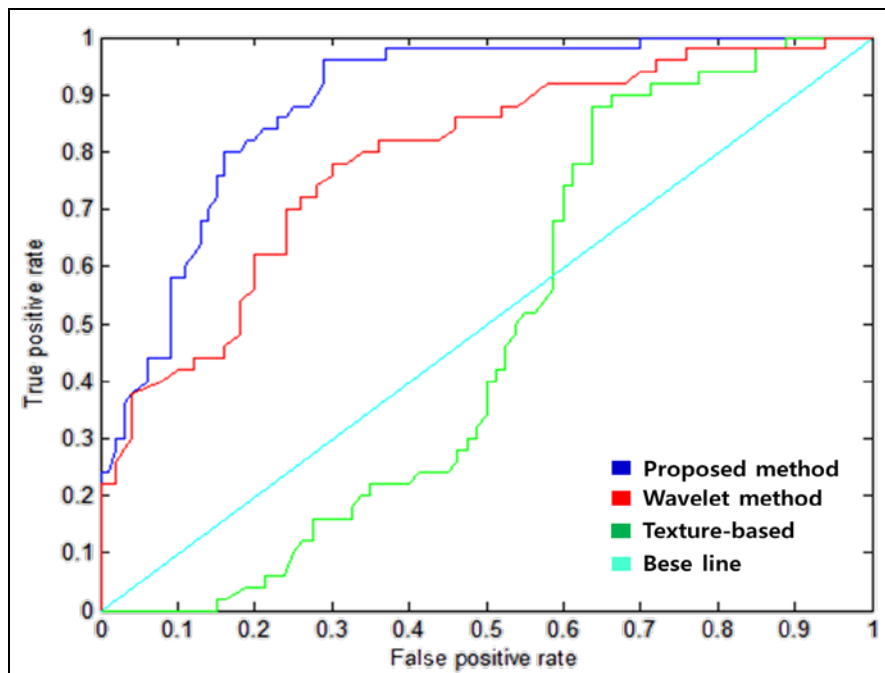


Fig. 12. ROC curve of overall analysis

## 5. Conclusion

This paper proposed an algorithm for overall similarity measurement considering medical image similarity measurement of a patient as a subsidiary method to increase the accuracy of patient information identification algorithm such as MPI, etc. The result of the experiment demonstrated that the proposed method is efficient as relatively higher accuracy is yield compared to the method in which the part using R2-map is processed with existing image information only. So we can check the R2 map information within the MR theory has been used to resolve the basic limitations in image processing. Proposed method did not stick to fundamental brightness, shapes recognition at calculating image similarity. The results have confirmed that the feature points, which have been detected through a corresponding R2 map, are meaningful; that is, the method in which the feature points detected through R2 map were used was more accurate than the conventional one in which the difference of pixel information was used. However, R2-map representing the distribution of iron component does not match if there is a large difference in image taking time. Therefore, the difference in image taking time can be seen as an important factor determining the accuracy of the proposed method. To solve

this problem, use of R2-map information of other body parts or use of another physical comparison information is required.

## References

- [1] Hyongsuk Moon, Kyhyun Um, "Design of Medical Image Retrieval System," *KORMARC*, pp.315-318, 2002.
- [2] S. Hemachande, A. Verma, S. Arora, and Prasanta K. Panigrahi, "Locally Adaptive Block Thresholding Method with Continuity Constraint," *Pattern Recognition Letters*, 28, pp. 119-124, 2007. [Article \(CrossRef Link\)](#)
- [3] C. C. Kang and W. J. Wang, "A Novel Edge Detection Method Based on Maximization of the Objective Function," *Pattern Recognition*, Vol. 40, No. 2, pp. 609-618, 2007. [Article \(CrossRef Link\)](#)
- [4] Rafael C. Gonzalez and Paul Wintz, "Digital Image Processing, Software Engineering A Practitiners' Approach," 3rd Ed., Addison-Wesley. Roger S. Pressman, 3rd Ed. McGraw Hill, 1993.
- [5] Haacke EM, Ayaz M, Khan A, et al, "Establishing a baseline phase behavior in magnetic resonance imaging to determine normal vs. abnormal iron content in the brain," *J Magn Reson Imaging* 26:256–64, 2007. [Article \(CrossRef Link\)](#)
- [6] Ogawa S, Lee TM, Kay AR, Tank DW, "Brain magnetic resonance imaging with contrast dependent on blood oxygenation," in *Proc of Natl Acad SciUSA*, 87:9868–9872, 1990. [Article \(CrossRef Link\)](#)
- [7] Ogawa S, Lee TM, "Magnetic resonance imaging of blood vessels at high fields: in vivo and in vitro measurements and image simulation," *Magn Reson Med*, 16:9–18, 1990. [Article \(CrossRef Link\)](#)
- [8] Ogawa S, Lee TM, Nayak AS, Glynn P., "Oxygenation-sensitive contrast in magnetic resonance image of rodent brain at high magnetic fields," *Magn Reson Med*, 14:68–78, 1990. [Article \(CrossRef Link\)](#)
- [9] Ogg RJ, Langston JW, Haacke EM, Steen RG, Taylor JS, "The correlation between phase shifts in gradient-echo MR images and regional brain iron concentration," *Magn Reson Imaging*, 17:1141–1148, 1999. [Article \(CrossRef Link\)](#)
- [10] Haacke, EM, Patrick JL, Lenz GW, Parrish T., "The separation of water and lipid components in the presence of field inhomogeneities," *Rev Magn Reson Med*, 1:123–154, 1986.
- [11] P.B. Kingsley, "Concepts in Magn," *Reson.*, 11, pp.29–49, 1999. [Article \(CrossRef Link\)](#)
- [12] E.M. Haacke, R.W. Brown, M.R. Thompson, R. Venkatesan, "Magnetic Resonance Imaging:Physical Principles and Sequence Design," *John Wiley & Sons Inc.*, USA., pp.129–133, 1999.
- [13] Reichenbach JR, Essig M, Haacke EM, Lee BC, Przetak C, Kaiser WA, Schad LR, "High resolution venography of the brain using magnetic resonance imaging," *MAGMA*, 6:62–69, 1998. [Article \(CrossRef Link\)](#)
- [14] Essig M, Reichenbach JR, Schad LR, Scho'nberg SO, Debus J, Kaiser WA, "High-resolution MR venography of cerebral arteriovenous malformations," *Magn Reson Imaging*, 17:1417–1425, 1999. [Article \(CrossRef Link\)](#)
- [15] Lee BCP, Vo KD, Kido DK, Mukherjee P, Reichenbach J, Lin W, Yoon MS, Haacke EM, "MR high-resolution blood oxygenation level-dependent venography of occult (low-flow) vascular lesions," *AJNR Am J Neuroradiol*, 20:1239–1242, 1999.
- [16] Tan IL, van Schijndel RA, Pouwels PJW, van Walderveen MAA,Reichenbach JR, Manoliu RA, Barkhof F, "MR venography of multiple sclerosis," *AJNR Am J Neuroradiol*, 21:1039–1042, 2000.
- [17] Fernandez-Seara MA, Techawiboonwong A, Detre JA, et al., "MR susceptometry for measuring global brain oxygen extraction," *Magn Reson Med*, 55:967–73, 2006. [Article \(CrossRef Link\)](#)

- [18] Baudendistel KT, Reichenbach JR, Metzner R, Schroeder J, Schad LR., "Comparison of functional venography and EPI-BOLD-fMRI at 1.5T," *Magn Reson Imaging*, 16:989–991, 1998. [Article \(CrossRef Link\)](#)
- [19] Reichenbach JR, Venkatesan R, Schillinger DJ, Kido DK, Haacke EM, "Small vessels in the human brain: MR venography with deoxyhemoglobin as an intrinsic contrast agent," *Radiology*, 204:272–277, 1997. [Article \(CrossRef Link\)](#)
- [20] S. Hemachande, A. Verma, S. Arora, and Prasanta K. Panigrahi, "Locally Adaptive Block Thresholding Method with Continuity Constraint," *Pattern Recognition Letters*, 28, pp. 119-124, 2007. [Article \(CrossRef Link\)](#)
- [21] J-L. Rose, C. Revol-Muller, M. Almajdub, E. Chereul, and C. Odet, "Shape prior integrated in an automated 3d region growing method," in *Proc. of Image Processing, 2007, ICIP 2007. IEEE International Conference on*, vol. 1, pp. 53- 56, 2007. [Article \(CrossRef Link\)](#)
- [22] M. Vetterli, J. Kovacevic, "Wavelets and Subband Coding," *Signal Processing*



**Sung-Jong Eun** received the Ph.D degree from Gachon University of South Korea in 2014 and the Research Professor both in Computer Science from Gachon University in 2014. His research areas include Computer Graphics, Medical image processing, Healthcare service, BCI, AR/VR/MR.



**Eun-Young Jung** received M.S. degree in Health Informatics, Gachon University, Korea, in 2001. She received Ph.D. degree of Medical Informatics from Ajou University, Korea, in 2012. She is currently manager of Health IT Research Center, Gachon University Gil Medical Center, Korea. Her research interests include u-healthcare, Telecare and Health IT, Virtual Reality simulation.



**Dong Kyun Park** received B.S. degree from College of Medicine, Chungbuk National University, Korea, in 1992. He received M.S. and Ph.D. degree in College of Medicine from Inha University, Korea, in 2000 and 2003. He is currently Director of Health IT Research Center and Medical Specialist of Gastroenterology in Gachon University Gil Medical Center, Korea. His research interests include u-healthcare, AI, and Big data analysis.



**Taeg Keun Whangbo** received the M.S. degree from City University of New York in 1988 and the Ph.D degree both in Computer Science from Stevens Institute of Technology in 1995. Currently, he is a professor in the Department of Interactive Media, Gachon University, Korea. He is also the Dean of Research Affairs in Gachon University. Before he joined the Gachon University, he was the software developer in Q-Systems which is located in New Jersey from 1988 to 1993. He was also the researcher in Samsung Electronics from 2005 to 2007. From 2006 to 2008, he was the president of the Association of Korea Cultural Technology. His research areas include Computer Graphics, HCI and AR/VR/MR.